Journal of Physics: Conference Series

PAPER • OPEN ACCESS

Influence of magnesium and strontium substitutions in the structure of hydroxyapatite lattice on the deposition rate and properties of the CaP coatings formed via RF-sputtering of the powder targets

To cite this article: A Y Fedotkin *et al* 2021 *J. Phys.: Conf. Ser.* **1799** 012008

Influence of magnesium and strontium substitutions in the structure of hydroxyapatite lattice on the deposition rate and properties of the CaP coatings formed via RF-sputtering of the powder targets

A Y Fedotkin[1], A I Kozelskaya[1], N M Korotchenko[2], A S Gigilev[2], E V Shesterikov[3] and S I Tverdokhlebov[1]

[1] Tomsk Polytechnic University, Tomsk, Russia
[2] Tomsk State University, Tomsk, Russia
[3] Institute of Atmospheric Optics V. E. Zuev SB RAS, Tomsk, Russia

E-mail: fedotkin_sasha@mail.ru

Abstract. This work is dedicated to studying of the properties of the calcium phosphate (CaP) coatings deposited on Ti substrates by radio-frequency magnetron sputtering (RFMS) of three hydroxyapatite-based powder targets: pure hydroxyapatite (HA), Mg-substituted HA (Mg-HA, Mg = 0.93 ± 0.13 at.%) and Sr-substituted HA (Sr-HA, Sr ~ 0.47 at.%). The influence of ionic substitutions in the structure of the sputtered targets on the surface morphology, physicochemical properties of the coatings and their wettability were studied. It is revealed that Mg and Sr ionic substitutions in the crystal lattice of HA at these concentrations don't affect deposition rate, however, it influences morphology, wettability and elemental and phase composition of deposited coatings.

1. Introduction

The most widely spread calcium phosphate (CaP) material used to cover metal implants for reconstructive surgery is hydroxyapatite (HA) because it is the base material of mineralized tissues of human bone, characterized by high bioactivity and osteoconductivity. Nowadays a lot of studies are dedicated to the influence of various ionic substitutions and dopes into the structure of HA on the structure and properties of coatings for biomedical applications [1]. Thus, it is shown that the presence of ionic substitutions contributes to bone renewal and remodeling.

The presence of Mg substitutions affects the metabolic activity of bone and its growth by affecting osteoblastic/osteoclastic cells. Lack of this element decreases the mechanical strength of bone and causes osteogenesis disorders [2]. Strontium is known as an element enhancing osteoblast activity and inhibiting osteoclasts [3].

Influence of Mg and Sr substitutions into the crystal lattice of β-tricalciumphosphate (TCP) powder targets on the deposition rate and properties of CaP coatings formed by RF-magnetron sputtering was studied in our previous work [4]. It was revealed that ionic substitutions cause significant changes in deposition rate, morphology, physicochemical and mechanical properties of coatings and their solubility. In this work, the effect of the same amount of Mg and Sr substitutions into HA powder target lattice on the deposition rate and properties of CaP coatings was studied.

2. Materials and methods

CaP coatings were deposited on Ti (VT6) discs with a 10 mm diameter and 1 mm thickness. Before coatings deposition, the substrates were exposed to mechanical treatment with grinding and polishing machine Unipol-802 (Zhengzhou TCH Instrument Co., Ltd, China). Coatings were also deposited on Si substrates to measure their thickness.

Three hydroxyapatite-based powders were used as the powder targets for RF-magnetron sputtering: pure hydroxyapatite (HA), Mg-substituted hydroxyapatite (Mg-HA) and Sr-substituted hydroxyapatite (Sr-HA). Concentrations of Mg and Sr substitutions were 0.93 ± 0.13 at.% and ~0.47 at.%, respectively. Powders production was carried out via liquid-phase synthesis.

Liquid phase synthesis of HA (1), MgHA (2), and SrHA (3) powders was carried out using a stoichiometric ratio Ca/P = 1.67((Ca+M)/P=1.67) and the following reaction equations [1]:

$$10Ca(NO_3)_2 + 6(NH_4)_2HPO_4 + 8NH_4OH = Ca_{10}(PO_4)_6(OH)_2 + 20NH_4NO_3 + 6H_2O \qquad (1)$$

$$9{,}37Ca(NO_3)_2 + 6(NH_4)_2HPO_4 + 0{,}63Mg(NO_3)_2 + 8NH_4OH \rightarrow$$
$$\rightarrow Ca_{9,37}Mg_{0,63}(PO_4)_6(OH)_2 + 20NH_4NO_3 + 6H_2O \qquad (2)$$

$$9{,}60Ca(NO_3)_2 + 6(NH_4)_2HPO_4 + 0{,}40Sr(NO_3)_2 + 8NH_4OH \rightarrow$$
$$\rightarrow Ca_{9,6}Sr_{0,4}(PO_4)_6(OH)_2 + 20NH_4NO_3 + 6H_2O \qquad (3)$$

To manufacture powder HA, an aqueous solution of calcium nitrate was mixed with a solution of ammonium hydrophosphate in concentrations of 0.5 M and 0.3 M, respectively. Mg and Sr substitutions were incorporated into the HA structure by adding magnesium or strontium nitrates into a solution of calcium nitrate. The aqueous solution of ammonia (25%, ρ = 0.9 g/ml) was used to reach a pH value of 10-11 in a solution of reactants. The reaction mixture was exposed to microwave irradiation of110 W for 40 minutes and left at room temperature for 48 hours. Then, precipitates were filtered, rinsed with a diluted solution of ethanol, and dried until constant weight (~ 15 h) at 90 ºC. Samples were treated by annealing at 800 °C for 4 hours.

The deposition process was carried out with the use of the upgraded universal magnetron sputtering system “Cathode-1M”. All the coatings were deposited under the same parameters: target/substrate distance – 40 mm, working pressure – 0.5 Pa, power density ~ 5.26 W/cm^2, deposition time – 7 hours.

Optical emission plasma spectra were measured with the spectroscope HR2000+ (OceanOptics, USA) in the wavelength range of 200-1000 nm. The integration time was 1s. Coating thicknesses were measured after its deposition using a mask on Si substrates applying contact profilometer Talysurf-5 (Taylor & Hobson, UK). The morphology of coatings was studied using atomic force microscopy (Solver-HV, NT-MDT, Russia). The elemental composition of the coatings was studied by energy dispersive spectroscopy (JSM-5900LV, JEOL Ltd., Japan). The study was conducted at a low vacuum and an accelerating voltage of 10 kV. The phase composition of the samples was studied using an XRD-6000 (Shimadzu, Japan) diffractometer using CuKα radiation. The phase composition analysis was carried out using PDF 4+ databases, as well as the POWDER CELL 2.4 full-profile analysis program.

A wettability study was carried out using the "sitting drop" method (EasyDrop, Krüss, Germany). Contact angles were determined for water, glycerol, and dimethylformamide. The volume of each droplet was 3 mL. Surface free energy (SFE) and its polar and dispersion components were determined by the OWRK method. The statistical reliability of the results was determined using a one-way analysis of variance and the Mann-Whitney U-test (Statistica 7.0, StatSoft, USA).

3. Results and discussion

Plasma discharges corresponding to sputtering processes of HA, Mg-HA and Sr-HA contain only the peaks of the working gas (Ar) and the atomic (Ca, P and O) and the molecular ions of the targets (CaO, PO, OH, H_2O, CaOH). Spectra don’t contain peaks corresponding to extra elements. The presence of H_2O ions is explained by the process of decomposition of the hydroxyl group of the HA target.

CaP coatings thicknesses formed by sputtering of HA, Mg-HA and Sr-HA powders were 1045 ± 55 nm, 912 ± 114 nm and 873 ± 80 nm, respectively. There is no statistically valuable difference between these results. It seems to us that the quantity of ionic substitutions is not enough to cause any change in the deposition rate. In our previous article [4], it's claimed that Mg substitutions in TCP lattice decrease the deposition rate of the CaP coatings, and, Sr ones, on the contrary, significantly increase it.

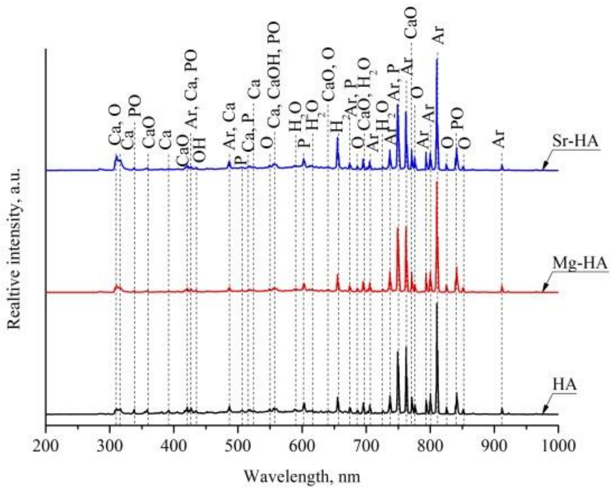

Figure 1. Plasma discharges corresponding to sputtering processes of HA, Mg-HA, and Sr-HA.

Multidirectional shallow traces on the initial substrate surface (figure 2a) caused by grinding and polishing are noticed. The surface of the coating formed by the sputtering of pure HA (figure 2b) is characterized by spherical grains with an area of 0.010 μm^2. There are no pronounced grains on the surface of CaP coating formed by the sputtering of Mg-HA (figure 2c). The surface of the coating formed by sputtering of Sr-HA (figure 2d) is represented with complex shape agglomerates consisting of grains with an area of 0.018 μm^2.

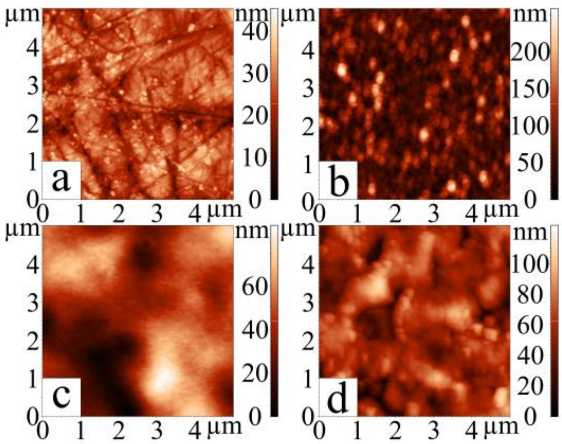

Figure 2. AFM-images of the surface of an initial substrate (**a**), the coating formed by sputtering of pure HA (**b**), the coatings formed by sputtering of Mg-HA (**c**) and Sr-HA (**d**).

All the coatings under study are characterized by the higher content of Ca and P and the lower content of O in comparison with the contents of the corresponding target (table 1). The content of Sr in the Sr-substituted target and the coating doesn't differ significantly, while the content of Mg in the coating is higher in the Mg-substituted target. Ti and Al in the content of coatings are explained by the content of the substrate.

HA-target is characterized with the closest value of Ca/P to stoichiometric HA (1.67), and the substituted targets have a lower value of this parameter. All the coatings have a lower value of Ca/P in comparison with the respective targets. CaP coatings formed by the sputtering of Mg-HA and Sr-HA are characterized by a similar Ca/P ratio.

Table 1. Elemental compositions of powder targets and coatings, at.%.

Sample	Ca	P	O	Mg	Sr	Ti	Al	Ca/P
Ti control	–	–	–	–	–	90.27 ± 0.42	9.73 ± 0.42	–
HA powder	13.80 ± 0.24	8.65 ± 0.49	77.54 ± 0.70	–	–	–	–	1.60 ± 0.07
HA coating	15.98 ± 0.07	12.12 ± 0.06	69.50 ± 0.16	–	–	2.22 ± 0.12	0.18 ± 0.03	1.32 ± 0.01
Mg-HA powder	11.85 ± 0.40*	9.02 ± 0.31	78.20 ± 0.04	0.93 ± 0.13*	–	–	–	1.32 ± 0.09*
Mg-HA coating	14.02 ± 0.75†	12.18 ± 0.68	71.30 ± 1.75†	1.35 ± 0.45†	–	0.80 ± 0.05†	0.35 ± 0.13†	1.15 ± 0.01†
Sr-HA powder	11.50 ± 0.39*	8.64 ± 0.12	79.38 ± 0.47*	–	~0.47*	–	–	1.33 ± 0.04*
Sr-HA coating	14.49 ± 0.09†	12.41 ± 0.08†	70.38 ± 0.47†	–	0.46 ± 0.02†	2.10 ± 0.48	0.17 ± 0.05	1.17 ± 0.01†

* significant difference with HA powder ($p<0.05$); † significant difference with HA coating ($p<0.05$).

XRD-study of the powder targets (figure 3a) revealed that the spectra of pure HA and Sr-substituted HA don't differ significantly. Mg-HA spectrum is characterized by the presence of peaks corresponding to whitlockite ($Ca_{2.59}Mg_{0.41}(PO_4)_2$). The content of Mg substitutions in the HA lattice is enough to cause the appearance of peaks of another phase in the spectrum.

XRD-spectra of the coatings under study (fiure 3b) are represented with the peaks corresponding to HA and Ti. The presence of Ti peaks is caused by the substrate material. For HA, Mg-HA and Sr-HA coatings, the peak at 25.85 deg. corresponds to a reflection of planes (002). Intensities of this peak are similar for HA and Sr-HA groups, but the peak corresponding to Sr-HA is wider, which indicates lower crystallinity of this group. This peak is also present in the XRD-spectrum of Mg-HA. However, it is wide and less intensive in comparison with other groups. Respectively, it is characterized by the lowest crystallinity. It can be concluded that both ion substitutions decrease the crystallinity of HA coatings. This conclusion is in agreement with the literature [1, 5] and the AFM results. The (002) orientation of the HA crystals is the most energetically beneficial in comparison with other ones [6]. This is in agreement with other results [7]. The HA peaks, corresponding to Mg-HA coating, are the lowest and the widest, which signifies the most amorphous structure among all other groups.

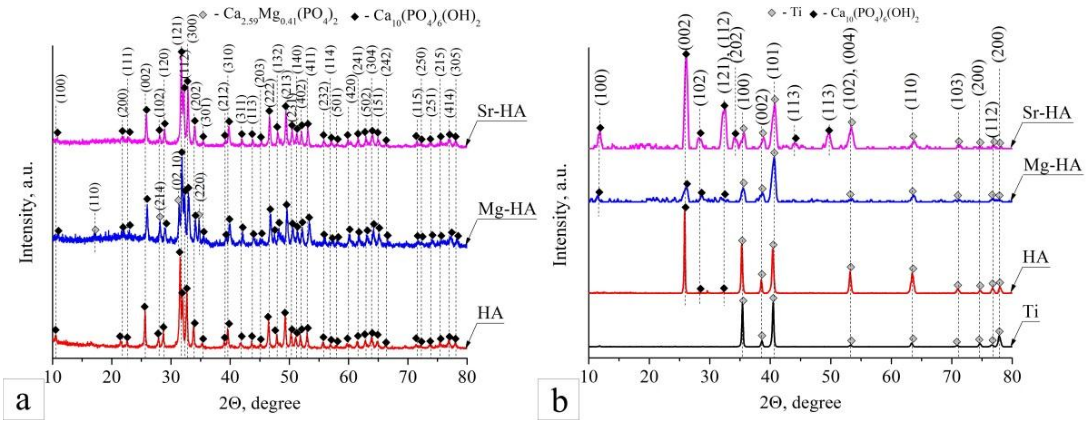

Figure 3. XRD-spectra of powder targets (**a**) and coatings (**b**).

The surface of CaP coatings formed by the RF-sputtering of HA-based targets is more hydrophilic in comparison with the initial substrate surface. Contact angles of the coatings under study with water don't differ significantly. However, CaP coatings with Mg substitutions have a slightly lower value of total SFE and its polar component and higher polar component than one formed by sputtering of pure HA. Sr substitutions have the opposite effect. The polar component of SFE is prevailing for all the coatings in comparison with the dispersive one. A high value of this component will induce better cell proliferation and promotes osseointegration [8].

Table 2. Contact angles of the coatings under study with water (θ_w), glycerin (θ_g) and dimethylformamide (θ_d), their total SFE (σ) and its dispersive (σ_D) and polar (σ_P) components.

Sample	θ_w, deg.	θ_g, deg.	θ_d, deg.	σ, mJ/m^2	σ_D, mJ/m^2	σ_P, mJ/m^2
Ti substrate	72.50 ± 3.88	61.10 ± 1.52	28.20 ± 0.73	34.39 ± 0.76	20.28 ± 0.33	14.12 ± 0.43
HA	47.90 ± 0.92	51.30 ± 2.05	43.30 ± 2.48	53.80 ± 0.79	6.09 ± 0.26	47.71 ± 0.53
Mg-HA	48.60 ± 1.28	49.50 ± 4.72	31.30 ± 3.64*	51.39 ± 1.32*	8.92 ± 0.52*	42.47 ± 0.80*
Sr-HA	44.40 ± 3.88	60.60 ± 2.10*	36.40 ± 3.83*	58.26 ± 1.67*	3.01 ± 0.31*	55.25 ± 1.36*

* significant difference with HA coating ($p<0.05$).

4. Conclusions

CaP coatings were formed on Ti substrates via RF-magnetron sputtering of HA-based powder targets. It was shown that Mg and Sr substitutions at these concentrations don't affect the deposition rate significantly. Morphologies of all coatings under study differ significantly. Coatings formed by sputtering of pure HA are characterized by a uniform surface with equiaxed grains, while the surface corresponding to Sr-HA is represented with an agglomeration of grains. The surface corresponding to Mg-HA is wavy without any structural elements. Whitlockite phases are present in the Mg-HA XRD spectrum. Ionic substitutions cause a decrease in the crystallinity and Ca/P ratio of coatings. Ca/P ratio of coatings is lower in comparison with corresponding targets. All the coatings surfaces under study are more hydrophilic than the surface of the initial substrate. The presence of Mg and Sr substitutions in the structure of CaP coatings allows stimulation bone formation and decrease bone resorption by suppressing of osteoclasts differentiation and their resorption activity. As a result, the balance between bone formation and its resorption moves to bone formation, which is especially important for patients with osteoporosis. Biomedical tests are planned.

Acknowledgments
This research was financially supported by Tomsk Polytechnic University Competitiveness Enhancement Program project VIU-SEC B.P. Veinberg-196/2020.

References

[1] Ratnayake J T B, Mucalo M and Dias G J 2016 *Journal of Biomedical Materials Research Part B: Applied Biomaterials* **105** 1–15
[2] Mróz W, Bombalska A, Burdyńska S, Jedyński M, Prokopiuk A, Budner B, Ślósarczyk A, Zima A, Menaszek E, Ścisłowska-Czarnecka A and Niedzielski K 2010 *Journal of Molecular Structure* **977** 145–52
[3] Šupová M 2015 *Ceramics International* **41** 9203–31
[4] Kozelskaya A I, Kulkova S E, Fedotkin A Y, Bolbasov E N, Zhukov Y M, Stipniece L, Bakulin A V, Useinov A S, Shesterikov E V, Locs J and Tverdokhlebov S I 2020 *Applied Surface Science* **509** 144763
[5] Ren F, Leng Y, Xin R and Ge X 2010 *Acta Biomaterialia* **6** 2787–96
[6] Filgueiras M R T, Mkhonto D and de Leeuw N H 2006 *Journal of Crystal Growth* **294** 60–8
[7] Fedotkin A Y, Bolbasov E N, Kozelskaya A I, Dubinenko G, Shesterikov E V, Ashrafov A and Tverdokhlebov S I 2019 *Materials Chemistry and Physics* **235** 121735
[8] Gittens R A, Scheideler L, Rupp F, Hyzy S L, Geis-Gerstorfer J, Schwartz Z and Boyan B D 2014 *Acta Biomaterialia* **10** 2907–18